

# Dissociation of Heavy Quarkonium in Quark-Gluon Plasma

Sidi C. Benzahra<sup>1</sup>, Benjamin F. Bayman<sup>2</sup>

<sup>1</sup> *North Dakota State University*

*Fargo, ND 58105, USA*

<sup>2</sup> *School of Physics and Astronomy, University of Minnesota*

*Minneapolis, MN 55455, USA*

## Abstract

In this work we calculate the lifetime of quarkonium moving with velocity  $v$  through a quark gluon plasma at temperature  $T$ . We also investigate the stability of heavy mesons with respect to the effects of color charge screening. An explicit, configuration-space potential is found for the screened interaction between the quarks constituting the meson. We solve the Schrödinger equation for the relative motion of the quarks in this non-spherical potential. In this way, we determine the range of  $v, T$  values for which the meson is bound. When a bound state exists, we use the bound-state wavefunction as the initial state for the dissociation of the meson due to gluon absorption. The meson lifetime is thus determined as a function of  $v$  and  $T$ , and conclusions are drawn concerning the possibility of detection of the meson in a high-energy heavy-nucleus collision.

## I. Introduction

Calculating the lifetime of a heavy meson in a medium of quarks and gluons is important for the understanding of the quark-gluon plasma. If a heavy-nucleus collision were to produce fewer than the number of mesons expected, we would need to ask about the lifetime of the meson in comparison with the lifetime of the quark-gluon plasma. If the lifetime of the quark-gluon plasma is greater than the lifetime of the meson in the quark-gluon plasma, one would think that there was probably a suppression of mesons due to the effect of screening or due to the effect of collision with gluons. In fact, many claim that suppression of  $J/\psi$  in heavy-ion collision could be a signature of quark-gluon plasma.

There is a relationship between the inverse screening length,  $m_{el}$ ; the number of flavors in the quark-gluon plasma,  $N_f$ ; and the temperature of the quark-gluon

plasma,  $T$ . If we increase the temperature of the quark-gluon plasma, the quarks and the gluons will become more active, and more effective at screening the interaction between a quark-antiquark pair. This relationship can be algebraically expressed [1] as follows:

$$m_{el}^2 = \frac{1}{3}g^2(N + \frac{N_f}{2})T^2, \quad (1)$$

where  $N = 3$  from the color  $SU(N = 3)$  group,  $g$  is the dimensional coupling constant of the field strength,  $F_a^{\mu\nu} = \partial^\mu A_a^\nu - \partial^\nu A_a^\mu - gf_{abc}A_b^\mu A_c^\nu$ , and  $N_f = 3$  is the number of light flavors in the quark-gluon plasma, which are the up, the down, and the strange quarks. We will also use the temperature-dependent running coupling constant of QCD, which is given by [1, 2]

$$\frac{g^2}{4\pi} = \frac{12\pi}{(11N - 2N_f) \log(T^2/\Lambda^2)}. \quad (2)$$

This equation explicitly displays asymptotic freedom:  $g^2 \rightarrow 0$  as  $T \rightarrow \infty$ . We notice that there is no intrinsic coupling “constant” on the right hand side of this equation. The only free parameter of the theory is the QCD energy scale,  $\Lambda$ , whose numerical value is dependent on the gauge and on the renormalization scheme chosen. If we choose the QCD energy scale to be  $\Lambda = 50$  MeV [1],  $N_f = 3$ , and  $N = 3$  we get

$$m_{el} = \frac{2\pi T}{\sqrt{3 \log(T/50)}}. \quad (3)$$

## II. Screened Potential

Chu and Matsui [3] studied the effects of Debye screening of the interaction between a heavy quark-antiquark pair moving through a quark-gluon plasma. For our purposes, their results may be summarized in the form of an effective in  $\vec{k}$  space quark-antiquark screened interaction:

$$V(k, \cos \theta_{\mathbf{k}}) = \frac{k^2 + A}{(k^2 + A)^2 + B^2}(1 - \gamma^2(1 - \zeta^2)) + \frac{k^2 + C}{(k^2 + C)^2 + D^2}\gamma^2(1 - \zeta^2), \quad (4)$$

where the quantities  $\zeta, A, B, C, D$  are defined in terms of  $\cos \theta_{\mathbf{k}} \equiv x$  by

$$\begin{aligned} \zeta &\equiv \frac{vx}{\sqrt{1 - v^2(1 - x^2)}} \\ A &\equiv \frac{1}{2}\zeta^2 + \frac{1}{4}(1 - \zeta^2)\zeta \log\left(\frac{1 + \zeta}{1 - \zeta}\right) \\ B &\equiv \frac{\pi}{4}(1 - \zeta^2)\zeta \\ C &\equiv (1 - \zeta^2)(1 - \frac{1}{2}\zeta \log\left(\frac{1 + \zeta}{1 - \zeta}\right)) \\ D &\equiv \frac{\pi}{2}(1 - \zeta^2)\zeta. \end{aligned}$$

$v$  is measured in units of  $c$ , and  $k$  is measured in units of  $m_{el}c/\hbar$ , the inverse Compton wavelength associated with the screening mass,  $m_{el}$ . The resulting interaction potential is given in units of  $\frac{4}{3}\alpha_s m_{el}c^2$ , with  $\alpha_s$  determined by QCD sum rules and lattice QCD calculations to be 0.232 [5]. The quantities  $\zeta, A, B, C, D$  defined here are non-negative in the integration region.  $V(\mathbf{k})$  is invariant under rotation about  $\hat{z}$ , and under reflection across the  $\hat{x} - \hat{y}$  plane.

We obtain the quark-antiquark  $\mathbf{r}$ -space interaction potential,  $U(\mathbf{r})$ , by Fourier transforming  $V(\mathbf{k})$ :

$$U(\mathbf{r}) = \frac{1}{2\pi^2} \int d^3k e^{i\mathbf{k}\cdot\mathbf{r}} V(\mathbf{k}) \quad (5)$$

In order to solve the quark-antiquark Schrödinger equation in  $\mathbf{r}$  space, we need an expansion of the interaction potential in the form

$$U(\mathbf{r}) = \sum_{\ell} u_{\ell}(r) P_{\ell}(\cos \theta_{\mathbf{r}}) \quad (6)$$

If we substitute the multipole expansion of the plane wave

$$\begin{aligned} e^{i\mathbf{k}\cdot\mathbf{r}} &= \sum_{\ell l} i^{\ell} (2\ell + 1) j_{\ell}(kr) P_{\ell}(\hat{k} \cdot \hat{r}) \\ &= 4\pi \sum_{\ell} i^{\ell} j_{\ell}(kr) \sum_{\mu} (Y_{\mu}^{\ell}(\hat{k}))^* Y_{\mu}^{\ell}(\hat{r}) \end{aligned}$$

into Equation (5), the axial symmetry of  $V(\mathbf{k})$  implies that only the  $\mu = 0$  terms will survive the  $\phi_{\mathbf{k}}$  integration. Comparison with Equation (6) yields

$$u_{\ell}(r) = i^{\ell} \frac{2}{\pi} (2\ell + 1) \int_0^1 dx P_{\ell}(x) \int_0^{\infty} k^2 dk j_{\ell}(kr) V(k, x). \quad (7)$$

The integration variable  $x$  in Equation (7) represents  $\cos \theta_{\mathbf{k}}$ . Because  $V(k, x)$ , given by Equation (4), is an even function of  $x$ , only even values of  $\ell$  will occur in the multipole expansion.

The  $k$ -integration in Equation (7) can be done exactly, using the theory of residues. We start with explicit expressions for the even- $\ell$  spherical Bessel functions:

$$j_{\ell}(kr) = \sum_{m=1,2,\dots,\ell+1} \frac{(\ell + m - 1)!}{(\ell - m + 1)! 2^{m-1} (m - 1)!} \times \frac{a_m^{\ell} \sin(kr) + b_m^{\ell} \cos(kr)}{(kr)^m} \quad (8)$$

with

$$\begin{aligned} a_m^{\ell} &\equiv (-1)^{\frac{\ell+1-m}{2}}, & b_m^{\ell} &\equiv 0 & \text{for odd } m \\ a_m^{\ell} &\equiv 0, & b_m^{\ell} &\equiv (-1)^{\frac{\ell+s-m}{2}} & \text{for even } m \end{aligned}$$

Individual terms of the sum in Equation (8) diverge as  $kr \rightarrow 0$ , but the entire sum converges as

$$\lim_{kr \rightarrow 0} j_{\ell}(kr) = \frac{(kr)^{\ell}}{(2\ell + 1)!!}$$

For the first term in Equation (4), we need the integral

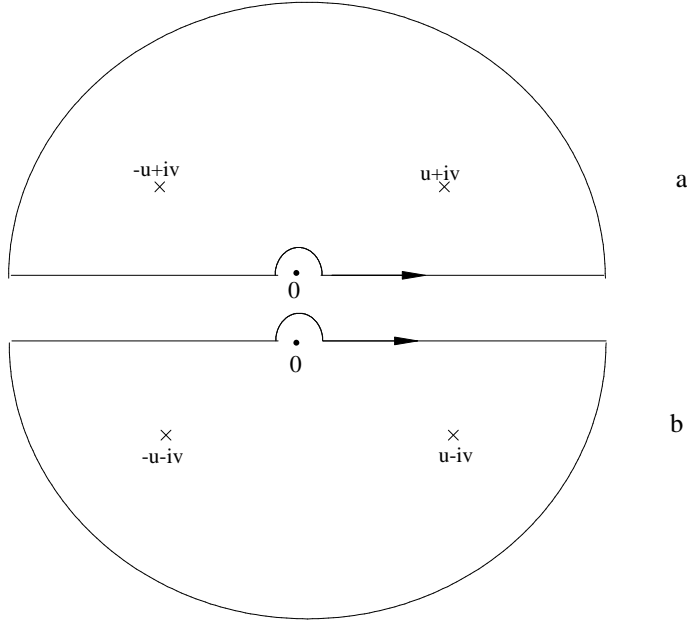
$$\begin{aligned}
I_\ell &\equiv \int_0^\infty k^2 dk \frac{k^2 + A}{(k^2 + A)^2 + B^2} j_\ell(kr) \quad (\text{even } \ell) \\
&= \frac{1}{2} \int_{-\infty}^\infty k^2 dk \frac{k^2 + A}{(k^2 + A)^2 + B^2} j_\ell(kr) \\
&= I_\ell^{(+)} + I_\ell^{(-)},
\end{aligned} \tag{9}$$

with

$$\begin{aligned}
I_\ell^{(+)} &= \frac{1}{4} \sum_{m=1}^{\ell+1} \frac{(\ell+m-1)!(-ia_m^\ell + b_m^\ell)}{(\ell-m+1)!2^{m-1}(m-1)!r^m} \int_{-\infty}^\infty \frac{e^{ikr}(k^2 + A)}{[(k^2 + A)^2 + B^2] k^{m-2}} dk \\
I_\ell^{(-)} &= \frac{1}{4} \sum_{m=1}^{\ell+1} \frac{(\ell+m-1)!(ia_m^\ell + b_m^\ell)}{(\ell-m+1)!2^{m-1}(m-1)!r^m} \int_{-\infty}^\infty \frac{e^{-ikr}(k^2 + A)}{[(k^2 + A)^2 + B^2] k^{m-2}} dk.
\end{aligned}$$

The contours used for the evaluation of these integrals are shown in Figures 1a and 1b. In both cases, the integrand is vanishingly small on the infinite semi-circular parts of the contours. On the real  $k$ -axis, and on the semicircle around  $k = 0$ , the sum of  $I_\ell^{(+)}$  and  $I_\ell^{(-)}$  gives us the convergent integrand we need for Equation (9). Thus we conclude that

$$\begin{aligned}
I_\ell &= 2\pi i \times [(\text{sum of residues at poles within the contour of Figure 1a}) - \\
&\quad (\text{sum of residues at poles within the contour of Figure 1b})]. \tag{10}
\end{aligned}$$



The poles within the contour of Figure 1a are at the zeroes of  $(k^2 + A)^2 + B^2$  with positive imaginary parts, *i.e* they are at  $\pm u + iv$ , where

$$u \equiv \sqrt{\frac{\sqrt{A^2 + B^2} - A}{2}}, \quad v \equiv \sqrt{\frac{\sqrt{A^2 + B^2} + A}{2}}.$$

The poles within the contour of Figure 1b are at  $\pm u - iv$ , and at  $k = 0$ . The final result is

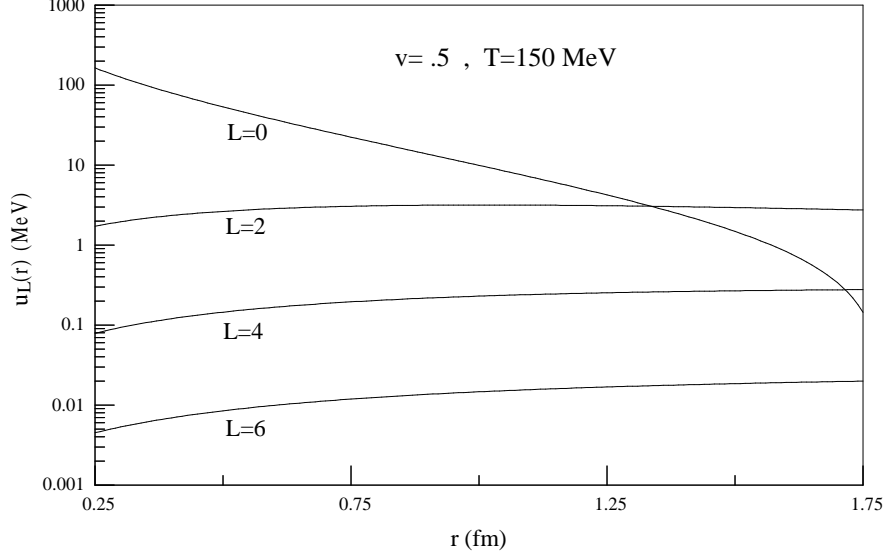
$$I_\ell = \frac{\pi}{2} e^{-vr} \sum_{m=1}^{\ell+1} \frac{(\ell + m - 1)! \left( a_m^\ell \cos(ur - (m - 1) \arctan \frac{v}{u}) - b_m^\ell \sin(ur - (m - 1) \arctan \frac{v}{u}) \right)}{(\ell - m + 1)! 2^{m-1} (m - 1)! (A^2 + B^2)^{\frac{m-1}{4}} r^m} + X_\ell, \quad (11)$$

where

$$\begin{aligned} X_0 &\equiv 0 \\ X_2 &\equiv \frac{\pi}{2} \frac{A}{A^2 + B^2} \frac{3}{r^3} \\ X_4 &\equiv \frac{\pi}{2} \left[ \frac{A}{A^2 + B^2} \frac{15}{2r^3} + \frac{B^2 - A^2}{(A^2 + B^2)^2} \frac{105}{r^5} \right] \\ X_6 &\equiv \frac{\pi}{2} \left[ \frac{A}{A^2 + B^2} \frac{105}{8r^3} + \frac{B^2 - A^2}{(A^2 + B^2)^2} \frac{945}{2r^5} + \frac{A(A^2 - 3B^2)}{(A^2 + B^2)^3} \frac{10395}{r^7} \right], \dots \text{etc} \end{aligned}$$

Here  $X_\ell$  represents the contribution to  $I_\ell^{(-)}$  of the residue at the  $k = 0$  pole.

The  $k$  integral for the second term in Equation (4) is performed in the same way. Finally, it is necessary to do the  $x$  integration in Equation (7). This must be done numerically. However, since the range is finite ( $0 \leq x \leq 1$ ) and the integrand is smooth, the integrand can be accurately performed with relatively few points. The  $x$ -integrations in the results shown below used Simpson's rule, with an  $x$ -interval of 0.001. An example of  $u_\ell(r)$ , for  $v = 0.5$  and  $T = 150 \text{ MeV}$ , is shown in Figure 2.



### III. Numerical Solutions of Schrödinger Equation

The binding energy of the quark and the antiquark can be calculated numerically by finding bound-state solutions of the Schrödinger equation. In this case, the non-relativistic Schrödinger equation governing the relative motion of the two quarks is written in the form

$$\left[ -\frac{\hbar^2}{2\mu} \nabla^2 + u_0(r) + u_2(r) P_2(\cos\theta) \right] \psi(r, \theta, \phi) = E \psi(r, \theta, \phi). \quad (12)$$

where  $\mu = m_Q/2$  is the reduced  $Q\bar{Q}$  mass. We have included only  $u_0(r)$  and  $u_2(r)$  in Equation (12) because, in the important  $r$ -region,  $u_\ell(r)$  with  $\ell > 2$  are negligibly small (see Figure 2). Because the potential is axially-symmetric, the eigenfunctions will be characterized by a definite  $m$ -value. However, the spherical symmetry of the potential is destroyed by the  $u_2(r)P_2(\cos\theta)$  term, and so the eigenfunctions will not be characterized by a unique value of the total angular momentum. Thus a solution must be constructed as a linear combination of total-angular-momentum eigenstates:

$$\psi(r, \theta, \phi) = \sum_{\ell} \frac{\phi_{\ell}(r)}{r} Y_m^{\ell}(\theta, \phi). \quad (13)$$

If this expansion is substituted into Equation (12) the result will be a set of coupled

second-order differential equations for the radial functions  $\phi_\ell(r)$ :

$$\left[ \frac{d^2}{dr^2} - \frac{\ell(\ell+1)}{r^2} - \frac{2\mu}{\hbar^2} u_0(r) - k^2 \right] \phi_\ell(r) - \frac{2\mu}{\hbar^2} \sqrt{\frac{4\pi}{5}} u_2(r) \sum_{\ell'} M_{\ell,\ell'} \phi_{\ell'}(r) = 0. \quad (14)$$

In Equation (14) we have introduced the notation

$$\begin{aligned} E &\equiv -\frac{\hbar^2}{2\mu} k^2 \\ M_{\ell,\ell'} &\equiv \int \sin\theta d\theta d\phi (Y_m^\ell(\theta, \phi))^* Y_0^2(\theta, \phi) Y_m^{\ell'}(\theta, \phi) \\ &= \sqrt{\frac{5(2\ell'+1)}{4\pi(2\ell+1)}} (2\ell' 0 m | \ell m) (2\ell' 0 0 | \ell 0). \end{aligned}$$

If we use explicit expressions for the vector-coupling coefficients, we obtain

$$\begin{aligned} M_{\ell,\ell'} &= \frac{1}{2\ell-1} \sqrt{\frac{45(\ell^2-m^2)((\ell-1)^2-m^2)}{16\pi(2\ell-3)(2\ell+1)}} \quad \text{if } \ell = \ell' + 2 \\ &= \sqrt{\frac{5}{4\pi}} \frac{\ell(\ell+1)-3m^2}{(2\ell-1)(2\ell+3)} \quad \text{if } \ell = \ell' \\ &= \frac{1}{2\ell'-1} \sqrt{\frac{45(\ell'^2-m^2)((\ell'-1)^2-m^2)}{16\pi(2\ell'-3)(2\ell'+1)}} \quad \text{if } \ell' = \ell + 2 \end{aligned}$$

In order to describe bound states of the meson we must find normalizeable solutions of the coupled equations (14) which are regular at  $r = 0$ . This defines an eigenvalue condition for  $k^2$ . A convenient numerical approach to this problem is suggested by the simple special case in which  $u_2(r) = 0$ . The coupling terms in Equation (14) vanish, leading to the single equation

$$\left[ \frac{d^2}{dr^2} - \frac{\ell(\ell+1)}{r^2} - \frac{2\mu}{\hbar^2} u_0(r) - k^2 \right] \phi_\ell(r) = 0. \quad (15)$$

We choose an arbitrary radius,  $R$ , and we guess a value for  $k^2$ . We then find an *interior* solution  $\phi_\ell^i(r)$  by numerically integrating Equation (15) from  $r = 0$  to  $r = R$ , starting at  $r = 0$  with the behavior

$$\phi_\ell^i(r) \xrightarrow{r \rightarrow 0} r^{\ell+1}. \quad (16)$$

Then we find an *exterior* solution  $\phi_\ell^e(r)$  by numerically integrating Equation (15) from a very large value of  $r$  down to  $r = R$ , starting at the large value of  $r$  with the behavior

$$\phi_\ell^e(r) \xrightarrow{r \rightarrow \infty} h_\ell^1(ikr). \quad (17)$$

The eigenvalue condition on  $k$  is that the relative normalizations of the interior and exterior functions can be chosen so that there is no discontinuity in value and slope

at  $r = R$ . This requires that their logarithmic derivatives at  $r = R$  be equal, which we can express as the condition

$$\frac{\phi_\ell^e(R)}{\phi_\ell^{e'}(R)} \frac{\phi_\ell^{i'}(R)}{\phi_\ell^i(R)} - 1 = 0. \quad (18)$$

$k^2$  in Equation (15) is varied until this condition is satisfied. The values of  $k^2$  so obtained are independent of the arbitrarily chosen  $R$ . This can be seen by using (15) to show that

$$0 = \phi_\ell^e \frac{d^2}{dr^2} \phi_\ell^i - \phi_\ell^i \frac{d^2}{dr^2} \phi_\ell^e = \frac{d}{dr} \left[ \phi_\ell^e \frac{d}{dr} \phi_\ell^i - \phi_\ell^i \frac{d}{dr} \phi_\ell^e \right], \quad (19)$$

so that  $\phi_\ell^e \frac{d}{dr} \phi_\ell^i - \phi_\ell^i \frac{d}{dr} \phi_\ell^e$  is independent of  $r$ , and so if (18) is true at one value of  $r$ , it is true at all  $r$ .

To generalize this procedure to the full set of coupled equations (14), we define sets of interior and exterior functions by

$$a_{\ell,\ell_1}(r) \xrightarrow{r \rightarrow 0} \delta_{\ell,\ell_1} r^{\ell+1} \quad (20)$$

$$b_{\ell,\ell_2}(r) \xrightarrow{r \rightarrow \infty} \delta_{\ell,\ell_2} h_\ell^1(ikr) \quad (21)$$

We now attempt to choose linear combinations of these interior and exterior functions

$$\phi_\ell^i(r) = \sum_{\ell_1} a_{\ell,\ell_1}(r) \alpha_{\ell_1} \quad (22)$$

$$\phi_\ell^e(r) = \sum_{\ell_2} b_{\ell,\ell_2}(r) \beta_{\ell_2} \quad (23)$$

in order to achieve continuity of value and derivative at the matching radius  $r = R$ . This requires that the coefficients  $\alpha_{\ell_1}$  and  $\beta_{\ell_2}$  satisfy

$$\sum_{\ell_1} a_{\ell,\ell_1}(R) \alpha_{\ell_1} = \sum_{\ell_2} b_{\ell,\ell_2}(R) \beta_{\ell_2} \quad (24)$$

$$\sum_{\ell_1} a'_{\ell,\ell_1}(R) \alpha_{\ell_1} = \sum_{\ell_2} b'_{\ell,\ell_2}(R) \beta_{\ell_2} \quad (25)$$

We can express this as a condition on the  $\beta_\ell$  alone by using Equation (24) to eliminate  $\alpha_{\ell_1}$  from Equation (25):

$$\alpha_{\ell_1} = \sum_{\ell_2} [a^{-1}(R) b(R)]_{\ell_1,\ell_2} \beta_{\ell_2} \quad (26)$$

$$\sum_{\ell_2} [b'^{-1}(R) a'(R) a^{-1}(R) b(R)]_{\ell_1,\ell_2} \beta_{\ell_2} = \beta_{\ell_1}. \quad (27)$$



The necessary and sufficient condition for a non-trivial solution to Equation (27) is

$$\det [ b'^{-1}(R) \ a'(R) \ a^{-1}(R) \ b(R) \ - \ \mathbf{1} ] = 0. \quad (28)$$

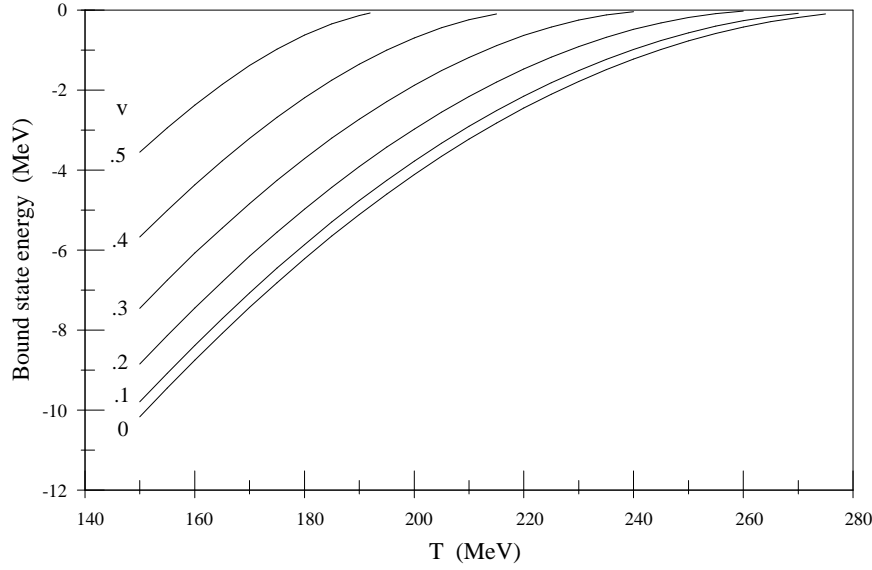
This is the multi-channel generalization of Equation (18). The value of  $k^2$  used in the numerical integration of the coupled equations (14) is varied until Equation (28) is satisfied to an acceptable accuracy. Then Equations (26) and (27) determine the  $\alpha_\ell$  and  $\beta_\ell$  up to an overall multiplicative factor, which can be obtained from the normalization condition

$$\sum_{\ell} \int_0^R dr [ \sum_{\ell_1} a_{\ell,\ell_1}(r) \alpha_{\ell_1} ]^2 + \sum_{\ell} \int_R^\infty dr [ \sum_{\ell_2} b_{\ell,\ell_2}(r) \beta_{\ell_2} ]^2 = 1. \quad (29)$$

As in the one-channel case, the consistency of the procedure guarantees that the calculated energy eigenvalues and eigenfunctions are independent of the choice of the matching radius.

The numerical integration of the coupled differential equations was performed using the 4th-order Runge-Kutta method with a step-length of 0.01 fm, starting at a minimum radius of 0.001 fm [4]. Although the  $\ell$  sum in Equation (14) has, in principle, no upper limit, the sum must be truncated in order to make the calculation finite. In the results to be shown below, the upper limit on  $\ell$  was taken to be 8. In fact, the strength of the coupling potential  $u_2(r)$  is small enough so that there was very little mixing of  $\ell \neq 0$  components into predominantly  $\ell = 0$  eigenfunctions.

The binding energies obtained in this way are plotted in Figure 3, as functions of  $v$  and  $T$ . Here we have used a heavy-quark mass of  $m_Q = 4.3 \text{ GeV}/c^2$ . It is seen that our calculations indicate that bound mesons cannot exist at temperatures greater than about  $T = 275 \text{ MeV}$ . Furthermore, at any given temperature, the binding energy is a decreasing function of  $v$ .



#### IV. Dissociation Time of a Heavy Meson Due To Collision With Thermal Gluons

Let us introduce the calculation of the dissociation time by asking: What is the rate of photo-ionization if we place a hydrogen atom in a cavity of thermalized photons at temperature  $T$ ? The Planck distribution [6] states that the flux of photons in the interval  $dk$  around  $k$  is

$$\frac{ck^2 dk}{\pi^2 [e^{\hbar kc/T} - 1]} . \quad (30)$$

Let  $\sigma(k)$  be the cross-section for photo-emission when the incident photon has momentum  $k$ . The rate for this process is then

$$R = \int_0^\infty \frac{ck^2 \sigma(k)}{\pi^2 [e^{\hbar kc/T} - 1]} dk . \quad (31)$$

According to Gasiorowicz, Quantum Physics, Chapter 24 [7]

$$\sigma(k) = \frac{V p_e e^2}{2\pi \hbar^3 m c^2 k} \int d\Omega \left| \int d^3 r \psi_f^*(\vec{r}) \hat{\epsilon} \cdot \vec{p} e^{ikz} \psi_i(\vec{r}) \right|^2 . \quad (32)$$

$\psi_i(\vec{r})$  is the normalized wave function of the initial bound electron state,  $p_e$  is the

asymptotic momentum of the outgoing electron [8], and  $m$  is its mass.

$$\psi_f(\vec{r}) \xrightarrow{r \rightarrow \infty} \frac{1}{\sqrt{V}} \left[ e^{i\vec{k}_e \cdot \vec{r}} + f(\theta', \phi') \frac{e^{-ik_e r}}{r} \right]. \quad (33)$$

$$\vec{k}_e = \frac{\vec{p}_e}{\hbar} = k_e [\sin\theta'(\cos\phi'\hat{x} + \sin\phi'\hat{y}) + \cos\theta'\hat{z}].$$

The  $d\Omega$  integration is over  $\theta', \phi'$ , the asymptotic direction of the outgoing electron.

Let us now consider the transition from QED to QCD. In QED the electron-photon vertex [9] is associated with matrix element of

$$ig_e \gamma^\mu = i\sqrt{\frac{4\pi e^2}{\hbar c}} \gamma^\mu. \quad (34)$$

In QCD the quark-gluon vertex [9] is associated with matrix element of

$$-i\frac{g_s}{2} \lambda^\alpha \gamma^\mu = -i\sqrt{\frac{4\pi\alpha_s}{2}} \lambda^\alpha \gamma^\mu. \quad (35)$$

The  $\lambda^\alpha$  is a generator of color SU(3). ( $\alpha = 1, 2, \dots, 8$ ). We are going from a meson (color singlet) to a  $Q\bar{Q}$  octet.

$$\langle [\text{octet}]_\alpha | \lambda^\alpha | [\text{singlet}] \rangle = \sqrt{\frac{8}{3}}.$$

Thus

$$i\sqrt{\frac{4\pi e^2}{\hbar c}} \longleftrightarrow -i\sqrt{\frac{4\pi\alpha_s}{2}} \sqrt{\frac{8}{3}},$$

which gives us

$$\frac{e^2}{\hbar c} \longleftrightarrow \frac{2}{3} \alpha_s$$

The photon flux density is multiplied by 8 to get the total gluon density (8 types of gluons, 8 generators of SU(3)). Finally,

$$R = \int_0^\infty \frac{8ck^2 \sigma(k)}{\pi^2 [e^{\hbar kc/T} - 1]} dk, \quad (36)$$

and

$$\sigma(k) = \frac{V p_Q \frac{2}{3} \alpha_s}{2\pi \hbar^2 \mu c k} \int d\Omega \left| \int d^3r \psi_f^*(\vec{r}) \hat{\epsilon} \cdot \vec{p} e^{ikz} \psi_i(\vec{r}) \right|^2, \quad (37)$$

where  $\mu$  is the reduced  $Q\bar{Q}$  mass.

In his evaluation of  $\sigma(k)$ , B. Muller [10] replaced  $e^{ikz}$  by 1 (long-wave-length approximation) and  $\psi_f(\vec{r})$  by  $e^{i\vec{k}_Q \cdot \vec{r}}$  (no distortion of the outgoing wave) and neglected

the connection between  $k_Q$  and  $k$ . We will make none of these approximations.

Now let us expand the final outgoing quark wavefunction

$$\psi_f(\vec{r}) = \frac{4\pi}{\sqrt{V}} \sum_{\ell} i^{\ell} e^{-i\delta_{\ell}} \sum_m Y_m^{\ell*}(\theta', \phi') Y_m^{\ell}(\theta, \phi) \frac{W_{\ell}(r)}{r}. \quad (38)$$

$$\begin{aligned} \hat{\epsilon} \cdot \vec{p} e^{ikz} \psi_i(\vec{r}) &= \frac{\hbar}{i} \hat{\epsilon} \cdot \vec{\nabla} e^{ikz} \psi_i(r) \\ &= \frac{\hbar}{i} e^{ikz} \hat{\epsilon} \cdot \vec{\nabla} \psi_i(r) \\ &= \frac{\hbar}{i} e^{ikz} \hat{\epsilon} \cdot \hat{r} \psi_i'(r) \end{aligned} \quad (39)$$

The last three equalities are satisfied since  $\hat{\epsilon} \cdot \hat{z} = 0$  (gluon has transverse polarization) and since  $\psi_i(\vec{r}) \approx \psi_i(r)$  (nearly spherically symmetric ground state). The  $W_{\ell}(r)$  are calculated using the methods of Section III.

Let

$$I(\vec{k}_Q) = \int d^3r \psi_f^*(\vec{r}) \hat{\epsilon} \cdot \vec{p} e^{ikz} \psi_i(\vec{r}), \quad (40)$$

which is the same as

$$I(\vec{k}_Q) = \frac{\hbar}{i} \frac{4\pi}{\sqrt{V}} \sum_{l,m} i^{-l} e^{i\delta_l} Y_m^l(\theta', \phi') \int d^3r Y_m^{l*}(\theta, \phi) \frac{W_l(r)}{r} \hat{\epsilon} \cdot \hat{r} e^{ikz} \psi_i'(r), \quad (41)$$

where

$$\hat{\epsilon} \cdot \hat{r} = \epsilon_x \sin\theta \cos\phi + \epsilon_y \sin\theta \sin\phi = \sqrt{\frac{2\pi}{3}} [-(\epsilon_x - i\epsilon_y) Y_1^1(\theta, \phi) + (\epsilon_x + i\epsilon_y) Y_{-1}^1(\theta, \phi)].$$

Now we use the relation

$$Y_{\pm 1}^1(\theta, \phi) e^{ikz} = \sqrt{\frac{3}{2}} \sum_{\ell} i^{\ell-1} \sqrt{\ell(2\ell+1)(\ell+1)} \frac{j_{\ell}(kr)}{kr} Y_{\pm 1}^{\ell}(\theta, \phi). \quad (42)$$

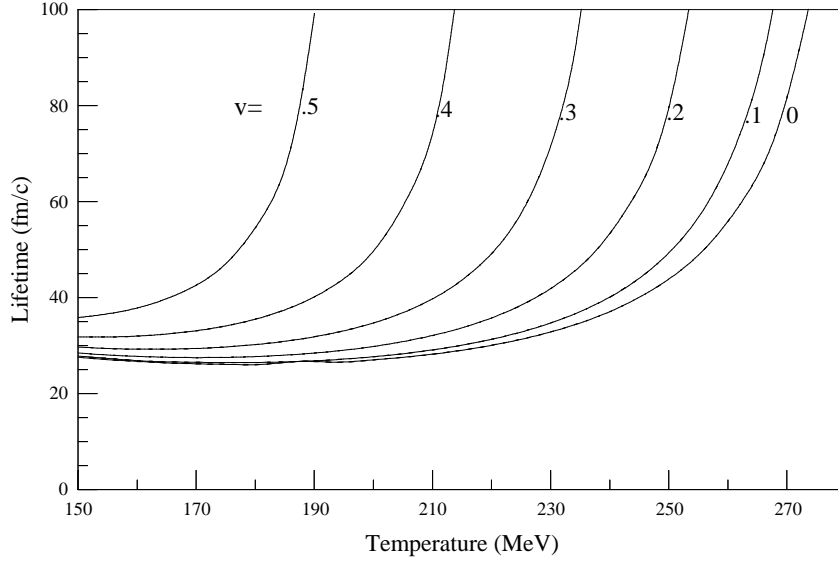
Substituting Equation (42) in Equation (41), we get

$$\begin{aligned} I(\vec{k}_Q) &= \frac{4\pi^{3/2}\hbar}{\sqrt{V}k} \sum_{\ell=1}^{Lmax} e^{i\delta_{\ell}} \sqrt{\ell(2\ell+1)(\ell+1)} \times \\ &\quad [(\epsilon_x - i\epsilon_y) Y_1^1(\theta', \phi') - (\epsilon_x + i\epsilon_y) Y_{-1}^1(\theta', \phi')] \int_0^{\infty} dr j_{\ell}(kr) W_{\ell}(r) \psi_i'(r). \end{aligned} \quad (43)$$

When we integrate over  $\theta'$  and  $\phi'$  (the  $d\Omega$  integration of Equation (37)), the orthonormality of the spherical harmonics converts the coherent sum over  $\ell$  in  $I(\vec{k}_Q)$  into an incoherent sum over  $\ell$  in  $\sigma(k)$

$$\sigma(k) = \frac{32}{3} \pi^2 \alpha_s \frac{\hbar c}{m_Q c^2} \frac{k_Q}{k^3} \sum_{\ell=1}^{Lmax} \ell(2\ell+1)(\ell+1) \left| \int_0^\infty dr j_\ell(kr) W_\ell(r) \psi'_i(r) \right|^2. \quad (44)$$

Equation (44) is inserted into Equation (36), and the integration over  $k$  is carried out numerically. Figure 4 shows a plot of calculated lifetime  $\tau = (1/R)$  as a function of  $T$  and  $v$ .



The most significant feature of Figure 4 is the prediction of a *minimum* lifetime. When  $T$  decreases below about  $T \sim 170$  MeV, the disintegration decreases because of falling gluon flux. As  $T$  increases above  $T \sim 170$  MeV, the disintegration rate decreases because of falling  $\sigma(k)$ . The maximum disintegration rate at  $T \sim 170$  MeV corresponds to a lifetime of  $\sim 27.5$  fm/c.

The decrease of  $\sigma(k)$ , in the important  $k$  region, with increasing  $T$ , is due to requirements of conservation of energy and momentum in a process in which a gluon is absorbed and a quark is emitted. For larger  $k$ , it is increasingly difficult to find, in the meson initial state, quark momenta that are large enough to satisfy both energy and momentum conservation. An analogous phenomenon occurs in the photoelectric effect, and results in photoelectric cross-sections that decrease with increasing photon momentum, once a threshold has been passed. In our situation, this effect is exacerbated by the decrease of meson binding energy with increasing temperature (Figure 3). This results in a meson wave function with greater spatial extent, and

thus a lower probability for the occurrence of the necessary high momentum components in the quark-antiquark wave function.

No lifetime minimum with respect to  $T$  was predicted by Muller [10] since he did not take into account both momentum and energy conservation. The expected lifetime of the quark gluon plasma is 10-20 fm/c, which is appreciably shorter than our minimum predicted meson-disintegration lifetime of 27.5 fm/c. Thus our conclusion is that the plasma will cease to exist before a significant fraction of the mesons will have been disintegrated by gluon impact. Therefore, this process will not have an appreciable effect on the number of mesons observed.

## V. Relation of Results to Experiment

Recent experiments [11] at the CERN SPS have shown a large suppression of  $J/\psi$  production in central Pb+Pb collisions. Following the original idea of Matsui and Satz [12] that  $J/\psi$  would be dissociated in a quark-gluon plasma due to color screening, the observed  $J/\psi$  suppression has been suggested as an evidence for the formation of the quark-gluon plasma in these collisions [13-15].

Since the  $\Upsilon$  meson states in a quark-gluon plasma are also sensitive to color screening [12, 16, 17], the study of the  $\Upsilon$  meson suppression in high energy heavy ion collisions can be used as a signature for the quark-gluon plasma as well. Because the binding energy of  $\Upsilon$  is larger than that of  $J/\psi$ , the critical energy density at which an upsilon meson is dissociated in the quark-gluon plasma is also higher [18]. One therefore expects to see the effects of the quark-gluon plasma on the production of the  $\Upsilon$  meson only in ultra-relativistic heavy ion collisions such as at the RHIC and the LHC. As in the case of  $J/\psi$ , one needs to understand the effects of the  $\Upsilon$  meson absorption in hadronic matter in order to use its suppression as a signal for the quark-gluon plasma in heavy ion collisions.

It is shown in Figure 3 that a bound  $\Upsilon$  meson cannot exist above a temperature of about 275 MeV, no matter what velocity it has relative to the plasma. Thus observation of  $\Upsilon$  mesons implies that the  $\geq 275$  MeV plasma never existed, or that the mesons were created in a plasma-free region. Bound  $\Upsilon$  mesons can exist at lower temperatures, even at speeds relative to the plasma that are an appreciable fraction of  $c$ . Thus the complete absence of  $\Upsilon$  mesons in a situation in which they should have been created is an indication of the existence of a  $T > 275$  MeV plasma.

In these considerations, it is not necessary to be concerned about dissociation of an  $\Upsilon$  meson due to absorption of a gluon, in a process analogous to the photoelectric effect or the photo-disintegration of the deuteron. Our calculations show that the lifetime of this process is longer than the expected lifetime of the plasma, so once a bound  $\Upsilon$  is formed, it has a high probability of surviving the collision.

## References

- [1] J.I. Kapusta, Finite Temperature Field Theory (Cambridge University Press, Cambridge, 1989).
- [2] J.I. Kapusta, Phys. Rev. D **46**, Number 10, 4749 (1992).
- [3] M.C.Chu and T. Matsui, Phys. Rev. D **39**, 1892 (1989).
- [4] Numerical Recipes in Fortran 97, William H. Press, Saul A. Teukolsky, William T. Vetterling and Brian P. Flannery, Second Edition, Chapter 16, Cambridge University Press, 1992 .
- [5] Matthias Jamin and Antonio Pich, Nucl. Phys. B **507** (1997) 334-352.
- [6] F. Reif, Fundamentals of Statistical and Thermal Physics (McGraw-Hill, Inc. Singapore, 1965).
- [7] S. Gasiorowicz, Quantum Mechanics Second Edition (John Wiley and Sons, Inc. 1996).
- [8] G. Breit and H. A. Bette, Phys. Rev. **93** (1954) 888 .
- [9] F. Halzen and A. Martin, Quarks and Leptons (John Wiley and Sons, Inc. 1984).
- [10] B. Muller, preprint nuc-th/9806023, v2 (unpublished).
- [11] M. Gonin *et al.*, the NA50 Collaboration, Nuc. Phys. A **610** (1996) 404c; M.C. Abreu *et al.*, the NA50 Collaboration, Phys. Lett. B **450** (1999) 456.
- [12] T. Matsui and H. Satz, Phys. Lett. B **178** (1986) 416.
- [13] J. -P. Blaizot and J.-Y. Ollitrault, Phys. Rev. Lett. **77** (1996) 1703.
- [14] C. -Y Wong, Nucl. Phys. A **630** (1998) 487.
- [15] D. Kharzeev, M. Nardi and H. Satz, Phys. Lett. B **405** (1997) 14; D. Kharzeev, C. Lourenco, M. Nardi and H. Satz, Z.
- [16] S. C. Benzahra, Phys. Rev. C **61** 064906 (2000).
- [17] For recent reviews, see, e.g., R. Vogt, Phys. Rept. **310** (1999) 197; H. Satz, Rept. Prog. Phys. **63** (2000) 1511.
- [18] F. Karsch, M.T. Mehr and H. Satz, Z. Phys. C **37** (1988) 617.

## Figure Captions

Figure 1. Contours for the evaluation of  $I^{(\pm)}$ .

Figure 2.  $u_\ell(r)$  for  $T = 150\text{MeV}$  and  $v = 0.5$

Figure 3. Calculated meson binding energies as a function of  $T$ , for various values of  $v$ .

Figure 4. Calculated meson dissociation lifetimes as a function of  $T$ , for various values of  $v$ .

## Acknowledgements

The authors would like to thank Joseph I. Kapusta for his very useful help.

Part of this work is supported by the U.S. Department of Energy under contract DE-AC03-76SF00098, and grant DE-FG02-87ER40328.